Available online at www.sciencedirect.com
SCIENCE DIRECT®
Analytica Chimica Acta 507 (2004) 95–105
ANALYTICA CHIMICA ACTA
www.elsevier.com/locate/aca

Design and development of microfabricated capillary electrophoresis devices with electrochemical detection

R.S. Keynton [a,*], T.J. Roussel, Jr. [a], M.M. Crain [b], D.J. Jackson [b], D.B. Franco [c], J.F. Naber [b], K.M. Walsh [b], R.P. Baldwin [c]

[a] *Department of Mechanical Engineering, University of Louisville, Louisville, KY 40292, USA*
[b] *Department of Electrical and Computer Engineering, University of Louisville, Louisville, KY 40292, USA*
[c] *Department of Chemistry, University of Louisville, Louisville, KY 40292, USA*

Received 25 August 2003; received in revised form 8 December 2003; accepted 17 December 2003

Abstract

Our efforts have been focused on developing a self-contained and transportable microfabricated electrophoresis (CE) system with integrated electrochemical detection (ED). The current prototype includes all necessary electrodes "on-chip" and utilizes miniaturized CE and ED supporting electronics custom designed for this purpose. State-of-the-art design/modeling tools and novel microfabrication procedures were used to create recessed platinum electrodes with complex geometries and the CE/ED device from two patterned ultra-flat glass substrates. The electrodes in the bottom substrate were formed by a self-aligned etch and deposition technique followed by a photolithographic lift-off process. The microchannels (20 μm deep × 65 μm wide (average)) were chemically etched into the top substrate followed by thermal bonding to complete the microchip device. CE/ED experiments were performed using 0.02 M phosphate buffer (pH 6), an analyte/buffer solution (2.2 mM dopamine, 2.3 mM catechol) and varying separation voltages (0–500 V) with a custom electronics unit interfaced to a laptop computer for data acquisition. Detection limits (S/N = 3) were found to be at the micromolar level and a linear detection response was observed up to millimolar concentrations for dopamine and catechol. The microchip CE/ED system injected 50 pl volumes of sample, which corresponded to mass detection limits on the order of 200 amol. For the first time, an integrated "on-chip" multi-electrode array CE/ED device was successfully designed, fabricated and tested. The majority of the electrodes (six out of eight) in the array were capable of detecting dopamine with the amplitude of the signal (i.e., peak heights) decreasing as the electrode distance from the channel exit increased.

Keywords: Capillary electrophoresis; Electrochemical detection; 'On-chip' integrated electrodes

1. Introduction

The construction of miniaturized "analytical laboratories" has led to major advancements in the field of instrument development, which can be primarily attributed to the crossover of microfabrication technology from the integrated circuit industry into analytical chemistry. This technological cross-fertilization has led to a dramatic increase in the number of devices where, the entire footprint of these miniaturized systems is approaching a size worthy of the title "lab-on-a-chip" (LOC) or "micro total analysis system" (μTAS) [1–3]. These studies have demonstrated the unique advantages for the LOC approach, including short analysis times, high separation efficiency, minute sample and reagent consumption, high sample throughput, and easy automation.

Fundamental to all methods of chemical analysis are the separation (isolation) and quantification (detection) of individual chemical species contained in a sample of interest. Of the separation methods employed in analytical chemistry, capillary electrophoresis (CE) has been the primary method investigated for integration onto microchip platforms. Early work involving chip-based electrophoresis devices almost exclusively utilized laser-induced fluorescence (LIF) detection. Examples of this method of detection on the LOC platform include the studies of separation of DNA and protein fragments [4–6], electrokinetic focusing [7–9], microchannel networks [10], and analyte/reagent mixing in microcapillaries [11–14]. LIF is extremely sensitive when combined with a point source light detector, such as a photomultiplier tube (PMT). However, a major limitation of this detection

* Corresponding author. Tel.: +1-502-852-6356; fax: +1-502-852-6053.
E-mail address: r0keyn01@gwise.louisville.edu (R.S. Keynton).

0003-2670/$ – see front matter © 2004 Elsevier B.V. All rights reserved.
doi:10.1016/j.aca.2003.12.042

technique is that many analytes are not inherently fluorescent and thus have to be "tagged" with a fluorescent molecule. Further, the instrumentation common to LIF makes this a distinctively off-chip methodology because of the bulky components that compose this detection system, including a confocal microscope, laser source, and the aforementioned PMT. Recent attempts have been made to scale down the fluorescent-based detection methodologies to a size that is more comparable to microfluidic platforms; however, none of the separated proteins were baseline resolved despite an apparent efficiency of 30,000 theoretical plates [15].

Another method of detection in CE, that has a strong potential for overcoming the limitations of LIF, is electrochemical detection (ED) since ED is more ideally suited for microfabrication processes. In particular, microelectrodes of different shape, size, and composition can be patterned onto glass, silica, and other substrates by the same photolithographic techniques used to fabricate the microchip's CE channels, thereby allowing the detection operation to be fully integrated onto the chip. Thus, with ED, there is no need for extensive off-chip detector components. Additionally, since ED requires only relatively simple electronics for control and data acquisition, the use of this detection approach should permit the entire CE/ED instrument to be miniaturized.

A number of research groups have investigated the implementation of ED on a microchip platform. Experimental devices have been constructed in glass [5,21–24], ceramics [25], polymers [26–36], and glass–polymer hybrid devices [31,37]. Current investigations indicate that the polymer-based materials have a lower natural zeta potential than silica-based materials and often require some type of surface modification, most commonly used direct chemical treatments or exposure to plasma, in order to increase the hydrophilic nature of the channel surface. It should be noted that, after such treatment, these alternative substrates often exhibit a short shelf life associated with their CE performance. Further, although these surface treatments have been shown to establish reasonable zeta potentials at the wall-fluid boundary, the resulting devices constructed from the modified substrates generally show smaller electrokinetic flow velocities than comparable devices created from glass or silica substrates [29–32].

ED in CE can be carried out either conductimetrically, potentiometrically or amperometrically. Conductimetric detection involves the application of an ac voltage to measure the conductance of the CE solution as it passes over a set of probes following separation [16,17]. The potentiometric detection technique involves coating the sensing electrode with an ion selective membrane and measuring the Nernst potential that develops across the membrane/solution interface as the analyte plug passes [17]. In amperometric detection, on the other hand, electrons are either consumed or liberated (depending on whether the analyte is oxidized or reduced); the resulting current is measured at the sensing electrode, where a specific electrical potential has been established against a reference electrode. Several excellent review articles have been published in the past 3 years [16–20], which discuss the most recent advances in the different ED modalities as well as the strengths and weaknesses of these approaches. Therefore, an in depth discussion of these modalities will not be presented in this article.

For both potentiometric and amperometric detection, three detection configurations are primarily employed with respect to the specific location of detection electrodes. These have been termed in-channel, off-channel detection, and end-channel detection [16]. A handful of devices using ED have been developed that are similar to an in-channel approach [26,27,39,40]. This configuration generally leads to bubble generation which can significantly decrease the signal-to-noise ratio of the ED signal. Additionally, the presence of the high electric field in the microchannel can significantly influence the resting background current generated at the surface of the working electrode. More recently, Martin et al. [40] employed an electrically isolated potentiostat in an in-channel electrode configuration to detect catechol. To date, only a few groups have been investigating the off-channel approach on a microchip platform [27,38,41]. The off-channel configuration is limited by the difficulties associated with fabrication of a fully-integrated device as well as discovery and placement of a suitable "decoupling" material. Most of the studies to date have developed ED systems that are analogous to end-channel CE [23,29,32,42–45]. Woolley et al. [42] were the first to explore amperometric ED within a microchip CE device using an end-channel approach, which utilized a photolithographically patterned working electrode and an externally applied/positioned Pt wire that was modified into a pseudo Ag/AgCl reference electrode.

To date, the work reported has primarily focused on the miniaturization of individual components such as the fluidic circuit or the electrodes rather than a holistic approach aimed at miniaturizing the entire system. In order to create a true LOC system, the electronics as well as the microfluidic circuit and detection scheme need to be miniaturized into a compact system. The purpose of this paper is to present an overview of this approach and, in particular, demonstrate some of the unique advantages of totally microfabricated systems designed for ED. In our work, we have employed a multidisciplinary approach to develop a self-contained and transportable CE/ED analysis system that (a) incorporates all necessary electrodes directly on the chip, and (b) utilizes miniaturized supporting electronics designed especially for the purpose of supporting our CE/ED microchip designs.

2. Experimental

2.1. Materials

Ultra-flat soda-lime glass was selected as the primary substrate since its surface characteristics naturally establish the requisite wall–buffer charge interface (zeta potential),

thereby eliminating the necessity for any chemical modification/treatment of the channel surfaces. This native solid–liquid interface is a fundamental requirement for establishing the electro-osmotic bulk flow of the buffer fluid in response to an applied electric field. To date, the majority of CE/ED devices developed employ end-channel detection since electrode placement inside the separation microchannel is problematic mostly due to bubble generation. Preliminary work in our lab also demonstrated this phenomenon, thus an end-channel detection scheme was selected for our device. Previous investigators utilized detection electrode geometries of either cylindrical (as in the case of the externally applied electrodes) or rectangular (generally associated with the photolithographically patterned electrodes). Utilizing microfabrication techniques, complex electrode patterns can be created to ensure an optimal fit of the design to the intended application. With this in mind, we wanted to incorporate an electrode shape that would optimize analyte detection. Intuitively, we concluded that the shape of the sample plug would change from an elongated rectangle to a crescent-shaped or radial-patterned plug upon exiting the channel. To verify this concept, computational modeling of the analyte plug shape after exiting the microchannel was performed by using a finite element (FE) software package (CoventorWare, Coventor, Raleigh, NC, USA). A two-dimensional computer model of the exit channel and detection reservoir was generated. The FE model used 27-node Manhattan brick elements (6.5 μm (W) × 10 μm (l)), with the width and length of the channel being 65 and 1000 μm, respectively, and the dimensions of the reservoir were 1000 μm × 1000 μm (Fig. 1a–c). Results from the finite element model clearly indicated that the rectangular plug exiting the separation microchannel transformed into a radial plug which radiated outwardly as it progressed further into the detection reservoir. Therefore, we designed detection electrodes that matched this radial shape in order to maximize the contact area with the analyte, thereby, increasing our signal-to-noise ratio.

Previous microchannel investigations performed by Jacobson and Ramsey [7] showed that by "focusing" an analyte stream in the intersection of the sample loading and separation microchannels, unwanted diffusion of analyte from the injection stream into the separation microchannel arm could be eliminated. Unfortunately, accomplishing this with an unbalanced microchannel system geometry (i.e., unequal arm lengths) requires multiple high-voltage (HV) power supplies, typically one for each terminating microchannel arm. To solve this problem, a "balanced-cross" microchannel pattern was developed, which consisted of four equal-length microchannel arms (10,000 μm), to simplify the electrical requirements for driving the electrokinetic flow. To reduce the "footprint" required by this geometry, two of the microchannel arms that make up the sample loading microchannel were bent at 90° (Fig. 2). Paegel et al. [46] demonstrated that bends in microfluidic channels distort an analyte plug with negative consequences for detection.

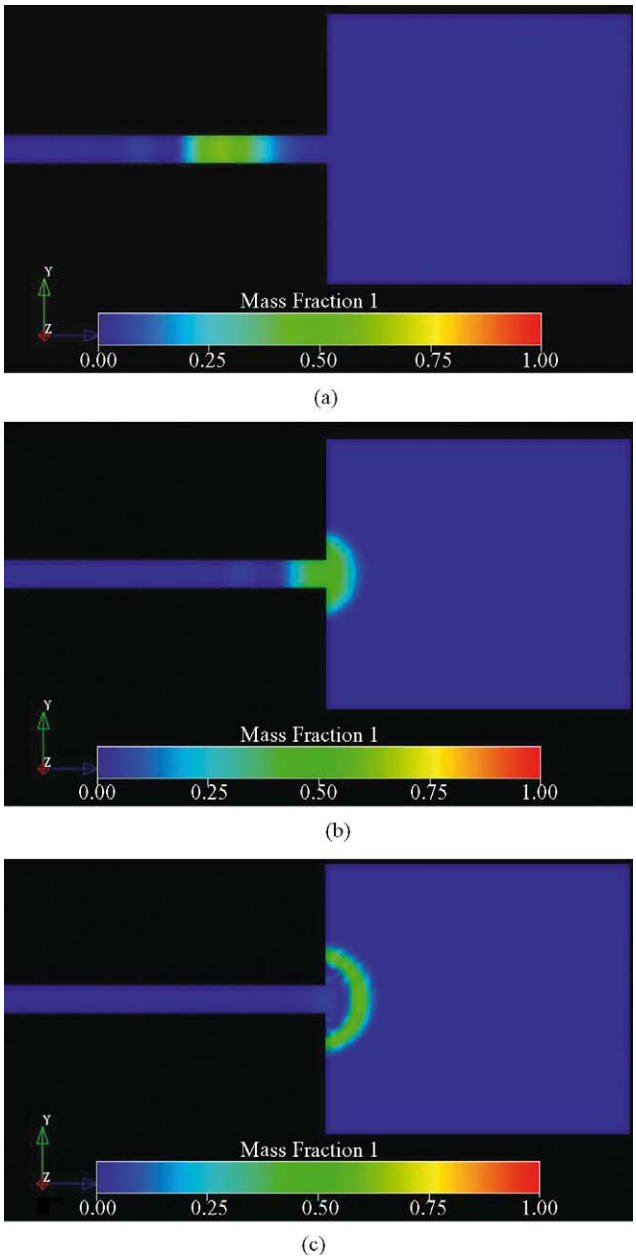

Fig. 1. Finite element model demonstrating plug shape (a) in the separation channel, (b) exiting the separation channel, and (c) in the detection reservoir.

However, the microchannels containing the 90° bends are utilized only during sample loading; and therefore, the plug integrity at the intersection is not compromised by either of these bends. This geometry simplifies the supporting electronics by allowing operation of the system with a single HV power supply described in detail below for both sample loading and injection/separation modes. The desired focusing of the sample stream with the pinching method at the microchannel system intersection would ultimately be accomplished with balanced currents in each arm. Computational modeling was again performed using FE analysis (CoventorWare, Coventor) to determine the appropriate

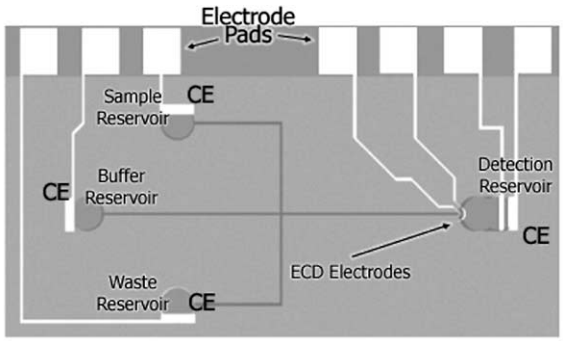

Fig. 2. Schematic of CE channel geometry and integrated electrode pattern design.

bias voltage level required to optimize the pinched sample plug geometry. For this simulation, a two-dimensional computer model of the channel intersection was generated. The FE model used 27-node Manhattan brick elements, with a minimum of 10 elements in the width dimension and 1000 elements along the length of the microchannel. Using a fixed length (1000 μm) and the average width of the channels (65 μm), the final model used contained 4800 elements and 460,870 nodes per arm (Fig. 3a and b).

2.2. Fabrication

The CE/ED device developed in this paper was constructed from two unexposed photomask blanks (5 cm × 3.5 cm; $t \approx 1524$ μm) that were comprised of ultra-flat, soda-lime glass pre-coated with a low reflective chrome and positive resist (supplied by Nanofilm, Westlake Village, CA, USA). These photomask blanks become the actual glass substrates, and the ultra-flat surface of the substrate permits the resolution and integrity of the fabricated features to be maintained, which are critical in the final bonding process. A detailed description of the fabrication process can be found in a chapter by Crain et al. [47], but a brief description will be provided here. In this fabrication procedure, the microfluidic circuit was machined in what will be referred to as the "top substrate" and the CE and ED electrodes were formed in the "bottom substrate". The microfluidic circuit was created in the top glass substrate (5 cm × 2.5 cm) using photolithography, bulk micromachining, and diamond glass drilling. After patterning, the microchannels were etched to a depth of 20 μm in a 6:1 buffered oxide etch solution. The final widths of the microchannels at the specified etch depth were 80 μm at the top and 50 μm at the bottom (65 μm wide (average)). To complete the fabrication of the top half of the microfluidic circuit, 5 mm diameter holes were drilled at the terminal ends of the etched microchannels using a drill press fitted with a diamond-tipped drill bit. In order to facilitate a larger detection reservoir volume, an extra hole was drilled, approximately one radius away from the original hole at the end of the detection microchannel. The extra hole acted to "diffuse" the build up of unreacted analyte and is also analogous to the "end-channel" ED approach.

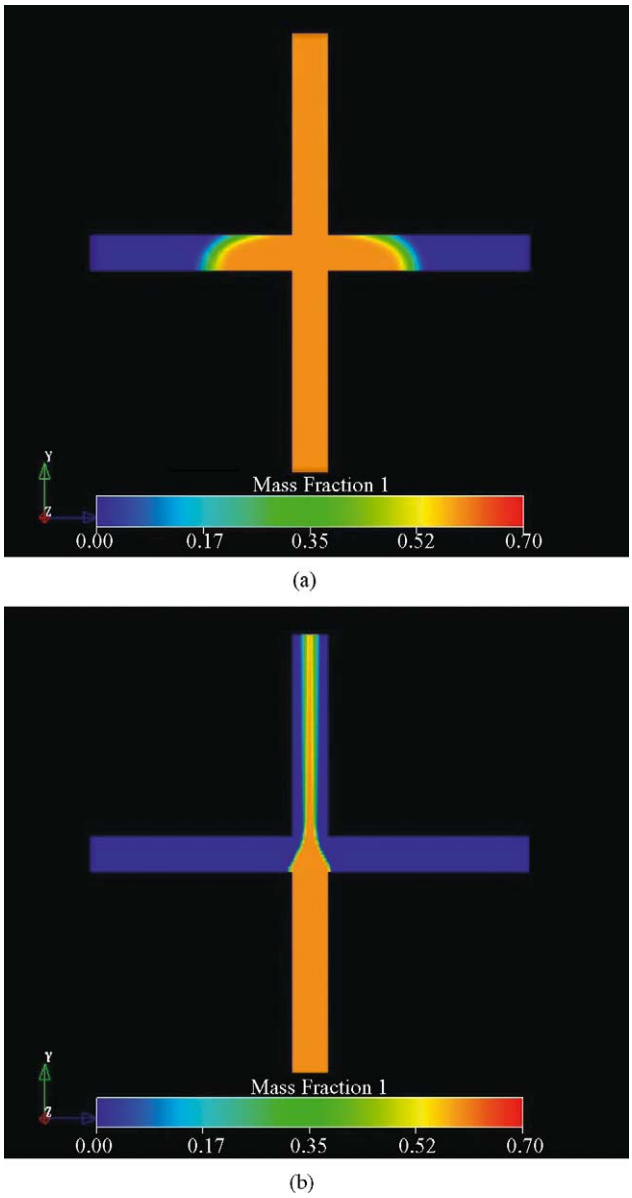

Fig. 3. Computer simulation of injection at the channel intersection when (a) no bias voltage is applied (i.e. floating), and (b) bias voltage (−250 V) is applied.

A novel fabrication process that yielded recessed platinum electrodes was developed to form both the detection and driving electrodes on the bottom substrate (5 cm × 3.5 cm). Specifically, the desired electrode configuration was patterned on the bottom substrate via traditional photolithography and the electrodes were formed by creating 0.3 μm recessions in the glass, using the existing chrome/photoresist layer as a masking layer with a self-aligned etch. After this etch step, titanium (thickness, $t = 10$ nm) followed by platinum ($t = 300$ nm) were RF and dc sputtered, respectively, onto the entire bottom substrate. The widths of the detection and reference electrodes were 40 μm, and this was the smallest electrode dimension used. A "lift-off" process was then used to remove the photoresist, which left only the

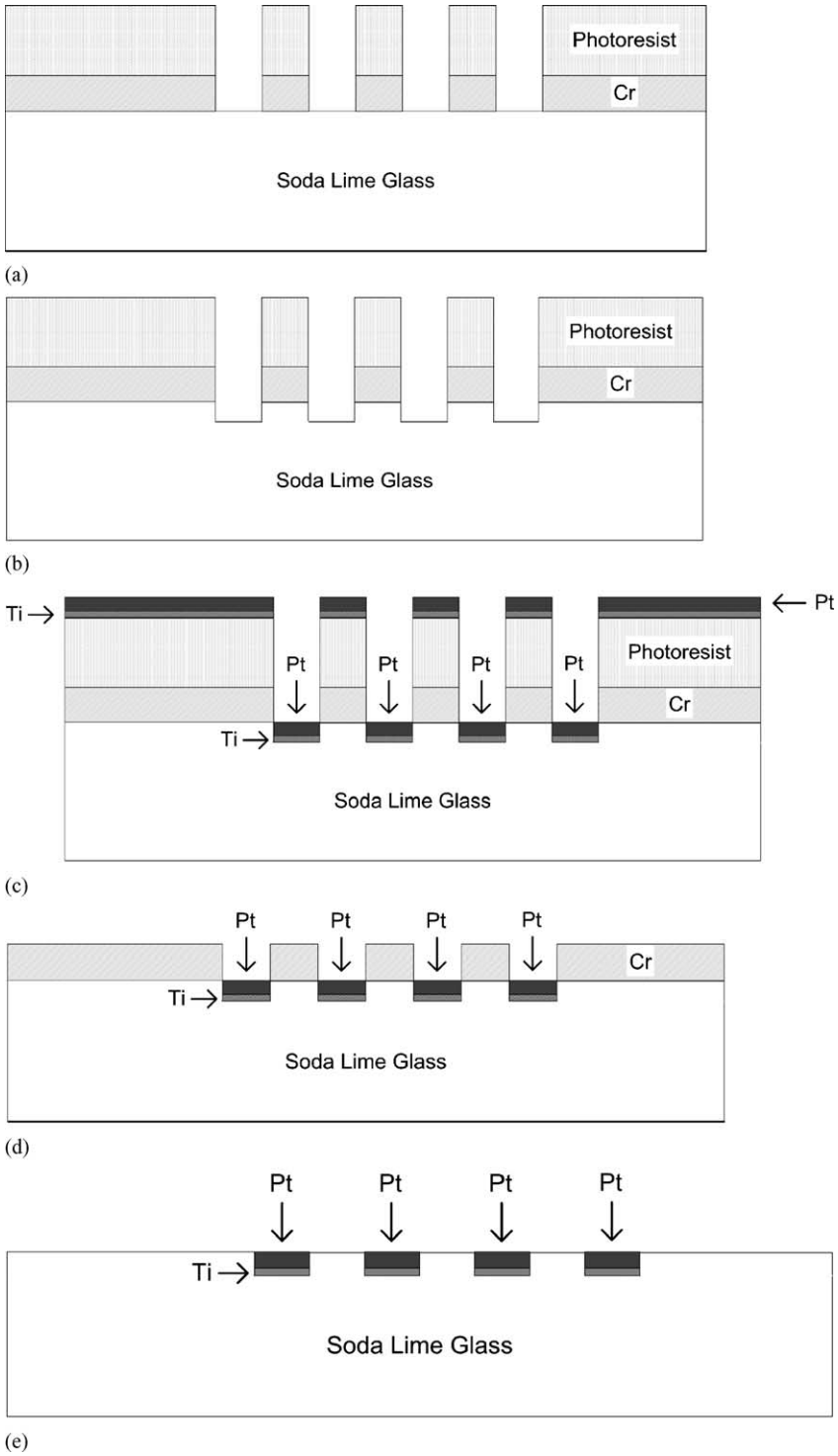

Fig. 4. Schematic of the microfabrication process flow for the bottom glass substrate, which includes (a) patterning of the positive resist and chrome layer, (b) etching of the 300 nm recessions, (c) sputter deposition of Ti and Pt, (d) lift off of the remaining photoresist, and (e) removal of the chrome layer.

recessed metal layers in their respective locations (Fig. 4a–e). Recession of the electrodes beneath the surface of the glass dramatically increased the fabrication yield by allowing a more conformal bond between the two glass surfaces, while the strategic design and placement of the ED electrodes contributed significantly to the microchip performance. Prior to bonding this substrate to the top substrate, the conductivity of each electrode was measured to confirm electrical continuity.

The two substrates were soaked in DI water for 15 min and then brought together under a stream of fresh DI water. While the two surfaces in contact were still wet, a

visual alignment process under high magnification (Leitz, Germany) was used to position the detection electrode near the end of the separation microchannel. Finally, thermal bonding of the CE device was accomplished by placing an alumina block on top of the aligned halves and increasing the temperature at 3 °C/min to 625 °C. This temperature was held constant for 30 min, followed by a ramp down to room temperature at 3 °C/min. It was imperative that the bond between the substrates be of sufficient strength to permanently seal the channel/capillary and electrically isolate the electrode leads between the two substrate layers.

2.3. Equipment

The portable, custom-made electronics consisted of a HV power supply (HVPS), interface circuit and an amperometric ED circuit. A detailed description of this HVPS, interface circuit and ED system has been previously reported [48], therefore, only a brief description will be provided here. The battery-powered, dual-source HV power supply employed Q12-5 and Q12-5N dc-to-dc converter modules (EMCO High Voltage Corporation, Sutter Creek, CA, USA) as HV sources. These modules are rated at +1.2 and −1.2 kV dc at a full load of 400 μA and are ideal for portable battery powered (four AA-size rechargeable 1300 mAh NiMH cells) operation because they are small (2.048 cm^3), lightweight (4.25 g), and require only 5 V dc of input voltage. In view of the nanoamp level currents encountered in microchip amperometric ED, a RC filter and copper foil shield were added to further reduce noise. In order to compensate for varying loads, battery discharge, and to make the output voltage adjustable, a closed loop regulation circuit was included for each source, and the power supply was connected to the CE chip through an interface circuit. The "balanced-cross" channel geometry simplified the design of the interface circuit and minimized the number of HV sources required since only the waste and buffer reservoirs were connected to the HV power supply. In addition, a stable pinched sample plug at the channel intersection was maintained without having to adjust the bias potential.

The CE microchip design incorporated two modes of operation: sample loading and injection/separation. In the sample loading mode, the buffer, sample and detection reservoirs were connected to the ground, which resulted in the buffer flowing from the three grounded reservoirs to the waste reservoir at equal rates since the electric fields were equivalent in each arm. This balanced-flow produced the desired pinched sample-flow at the channel intersection and prevented sample leakage into the detection or buffer channels. In the injection/separation mode, the positive HV source was connected to the buffer reservoir and only the detection reservoir remained at ground potential, while the sample and waste reservoirs were at a reduced potential. This reduced field primarily directed buffer flow from the buffer reservoir towards the detection reservoir with a smaller flow to the waste and sample reservoirs, which again prevented leakage of sample into the detection channel.

A potentiostat circuit and transimpedance (current-to-voltage) amplifier comprised the amperometric ED electronics. Both circuits used common operational amplifier integrated circuits (ICs) powered by a single 9 V battery whose output was split to provide a bipolar voltage source. A TLC2202 (Texas Instruments, Dallas, TX, USA) operational amplifier (acting as a single stage transimpedance amplifier) maintained the working electrode at ground potential, and a potentiometer was connected to the amplifier input to compensate for offset currents. An on-board potentiometer or external control signal was used to adjust the reservoir versus working electrode potential over a range of ±2 V. The power supply and interface circuit were controlled with a National Instruments (Austin, TX, USA) model DAQ 500 input–output (I/O) card and LabVIEW software and 50 samples/s were recorded from the ammeter using the National Instruments I/O card and customized LabVIEW software.

2.4. Procedures

The CE microchip was placed onto a custom-made acrylic platform with spring loaded contact leads in order to secure the small CE system during testing and provide an easy method of connecting the "on-chip" electrodes to the driving and sensing electronics. Prior to testing, the capillaries were filled via capillary action with buffer solution (sodium phosphate, 20 mM, pH 6.1). Approximately 2 ml of two neurotransmitters, dopamine (MW = 189.64; 2.2 mM) and catechol (MW = 110.11; 2.3 mM), both in the buffer solution, were placed in the sample reservoir. Both analytes are electrochemically active at the buffer pH used and were baseline resolved at all values of the applied electric field range (0–225 V/cm). Additionally, dopamine is positively charged in this buffer, while catechol is effectively neutral and acted as a neutral marker for quantifying the electro-osmotic flow.

Various experiments were performed on the microfabricated prototype devices involved changing the applied ED electrode, the sample loading and the separation voltages. In the standard three-electrode detection cell, knowledge of the half-cell potential for the oxidation or reduction of a species allows some control over the detection selectivity of an ED experiment. In order to verify oxidation potentials and perhaps gain insight as to whether the CE field would influence detection, hydrodynamic voltammograms were obtained by adjusting the applied reference voltage from −0.250 to +1200 mV in 50 mV increments. To observe the effects of increasing sample loading voltage on the focused injection stream, the injection voltages were varied (from 0 to 250 V). The results were examined for variations in elution time as well as changes in the area under the curves produced by the detection circuit. To investigate the separation of individual species in a sample plug with the prototype, a range of CE voltages (0 to −500 V) were used

to separate the analytes dopamine and catechol. This CE voltage range produced fields in the range of 0–225 V/cm. Post-processing of the data included performing a moving window average on 50 samples of data recorded by the DAQ system using Mathcad software (MathSoft, Cambridge, MA, USA). While the advanced (eight-electrode) microchip device theoretically allows for simultaneous ED at each working electrode, the electronics were designed to record data for a system with only one working electrode. Thus, the performance of the eight-electrode device was evaluated by changing the working electrode between each experiment.

3. Results and discussion

A photograph of our intact CE microchip device is shown in Fig. 5. Also, included is a magnified view showing a basic two electrode ED configuration that was fabricated and employed during the first phase of this work. One of the great attractions of the microfabrication approach, from the ED point of view, is that photolithographic patterning allows absolute control over fundamental electrode features including size, shape, and location on the chip. (Another important electrode feature, its composition, is also variable via microfabrication; but this possibility was not investigated in the current work.) In general, photolithographic patterning should be able to produce electrode structures consistently down to the 5 μm level. However, with the transparency-based photomasks prepared in-house and used here, the structure size limit was restricted to a minimum of 30 μm.

The simple configuration illustrated in Fig. 5b shows an arrangement in which two 40 μm wide Pt "finger" electrodes were sputtered onto the bottom glass substrate with an inter-electrode distance of 80 μm and then positioned near the CE channel outlet. This specific design was chosen in order to provide preliminary experimental insight into the effect of working electrode placement on ED performance and the possibility of fabricating a working electrode/reference electrode pair in close proximity. In particular, the crescent

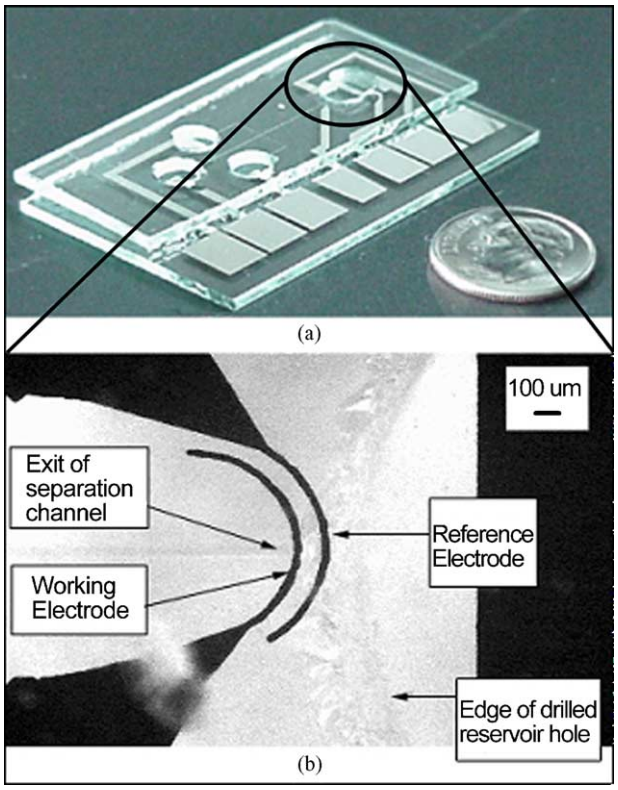

Fig. 5. Photographs of (a) entire CE/ED microchip and (b) magnified (30×) top view of the ED cell and electrodes.

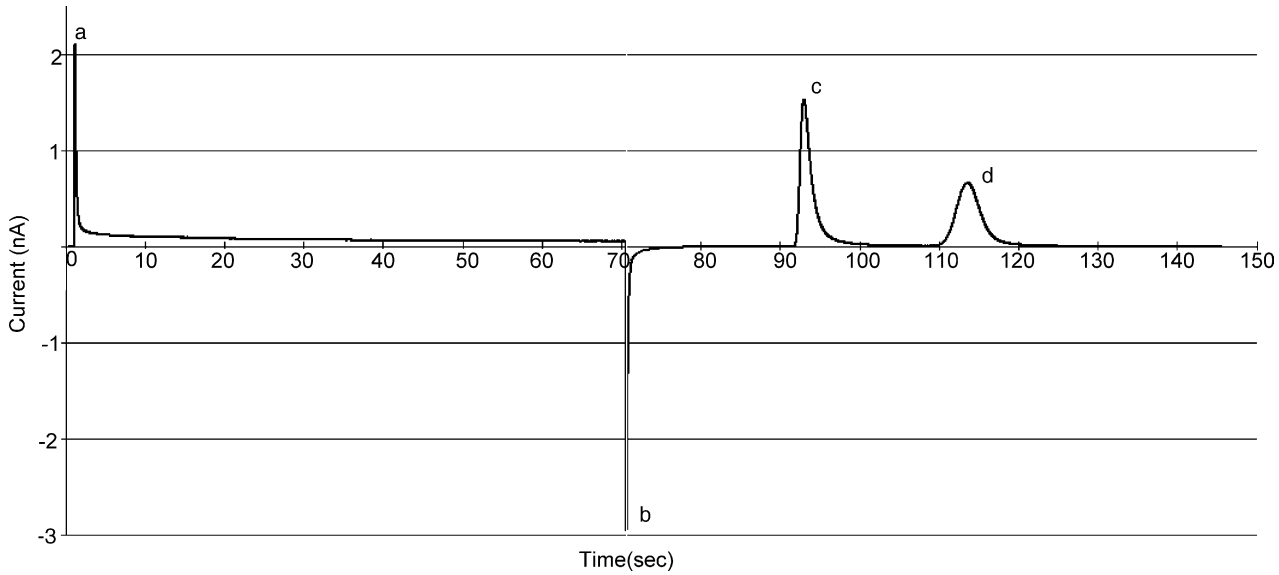

Fig. 6. Plot of the electrical output signal for an entire CE/ED run, where the spikes are the current at the working electrode for: (a) sample loading, (b) sample injection/separation, (c) dopamine detection, and (d) catechol detection.

shape of the electrodes was intentionally selected in order to mimic the shape of an analyte plug, predicted in the modeling calculations (see Fig. 1), as it exited the CE channel and started to diffuse toward the detection reservoir. The more complex device configuration shown in Fig. 7b contains eight Pt "half-finger" electrodes (four to the left and four to the right of the CE channel) at various distances out into the detection reservoir. In this case, the spacing between opposing electrodes in each pair was 10 μm. This particular design would allow a more precise evaluation of the effect of CE exit-working electrode distance on microchip performance and could also serve as a prototype for a more sophisticated device containing an array of ED sensors. Both of these designs were employed in the work described below.

Fig. 6 illustrates the data obtained for a complete working cycle comprising both sample loading and injection/separation operations. The detector configuration used was similar to the two-electrode arrangement shown in Fig. 5b with the inner Pt finger (W1) serving as the working electrode and the outer (W2) as the reference (or pseudo-reference). The sample consisted of a mixture of the model electroactive analytes, dopamine and catechol. What is plotted in the figure is the working electrode signal (i.e., current) occurring throughout the entire measurement process. At point A, a HV was applied to the CE electrode in the waste reservoir on the microchip to initiate solution flow from the sample well. (As described earlier in Section 2.3, equal flow actually occurs from the sample, buffer, and detection reservoirs in order to create a pinched sample-flow and prevent leakage into the separation channel.) In this particular experiment, the HV was applied for a total of 70 s during which time sample solution was continuously directed across the channel intersection and into the waste reservoir. Interestingly, after the initial spike in the working electrode current following application of the HV to the waste reservoir, the signal rapidly settled down to a low, nearly constant baseline on the order of only 0.1 nA. At point B, the HV was removed from the waste reservoir and applied between the CE electrodes in the buffer and detection chambers so that the sample solution present in the channel intersection was injected into the separation channel as a well-defined plug. At this stage, the CE separation of the sample components commenced, with the positively charged dopamine (C) migrating toward the detection reservoir, faster than the neutral catechol (D). Again, after the initial current spike that occurred upon HV switching, the ED current rapidly settled down to a low steady-state background level. After the final sample component left the separation channel and passed into the detection reservoir, a new cycle of sample loading and injection/separation could be repeated by appropriate HV manipulation.

The analytical performance of our CE/ED microchip (with ED electrodes as in Fig. 5b) has been described previously [24,48]. Detection limits (signal/noise = 3) for dopamine and catechol were found to be at the μM level with the linear range extending up to mM concentrations. Taking into account the roughly 50 pl injection volume employed, this corresponds to the mass detection limits on the order of 200 amol. Most important, the microchips themselves have proven extremely durable, with the microfabricated ED electrodes providing stable analytical response over months of usage and hundreds of individual sample injections.

As indicated above, a unique aspect of the microfabrication approach is that microchips containing complex ED configurations capable of relatively sophisticated applications can be prepared with no more effort or expense than those with very simple electrode patterns. Thus, once the appropriate photomask has been created, a chip containing any desired electrode pattern can be prepared by exactly the same procedure as used above. In fact, the over-all dimensions of our devices are small enough that four separate devices are patterned and fabricated simultaneously on the same glass substrate (and subsequently separated from one another manually with a dicing saw). Depending on the

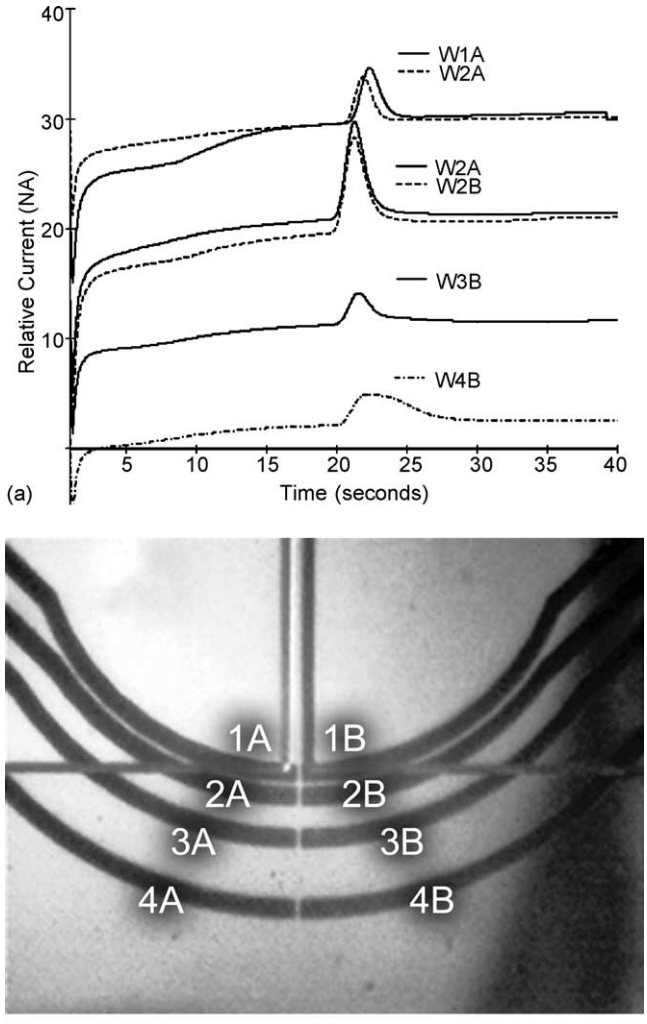

Fig. 7. Eight-electrode ED configuration when all the electrodes are under the "shelf": (a) dopamine output currents from six of eight electrodes, and (b) photograph of the electrode fingers at the channel exit.

mask employed, these could be four replicate devices containing the same electrode configuration or four completely different designs.

Interesting results obtained with an eight-electrode ED configuration are illustrated in Fig. 7. This device contained eight Pt "half-finger" electrodes (four to the left and four to the right of the CE channel) at various distances out into the detection reservoir: W1A and W1B, at the CE channel exit; W2A and W2B, approximately 10 μm away from the CE exit; W3A and W3B, approximately 50 μm away; and W4A and W4B, approximately 100 μm away. In this case, the spacing between the left and right electrodes in each pair was only 10 μm. This particular design allowed a more precise evaluation of the effect of CE exit-working electrode distance on microchip performance and could also serve as a prototype for a more sophisticated device containing an array of independent ED sensors. In this set of experiments illustrated here, each of the eight electrodes was used in turn as the ED working electrode for the detection of dopamine. (Note that only the injection/separation stage of each experiment is shown.) Unfortunately, for this microchip, electrodes W3A and W4A failed to give any electrical response at all; and, therefore, no electropherograms are shown for these two. This type of problem in which one or more electrodes failed to survive the microfabrication and wafer bonding processes was not an uncommon occurrence during our earlier fabrication efforts and was presumably due to sub-microscopic breaks or "open-circuits" in the 300 nm thick Pt films used to form both the electrodes themselves and their electrical contacts, sometimes a few cm in length, to the microchip edge. However, as our experience level has increased, such failures have become increasingly rare.

It is clear from Fig. 7a that all six of the active electrodes yielded qualitatively similar electropherograms, each containing a single oxidation peak for dopamine with a migration time in the 20–25 s range. The current levels seen were greatest for the W2 electrode pair presumably because (1) the exposed areas of electrodes W1A and W1B were substantially smaller and (2) electrodes W3B and W4B were situated far enough away from the channel exit so that

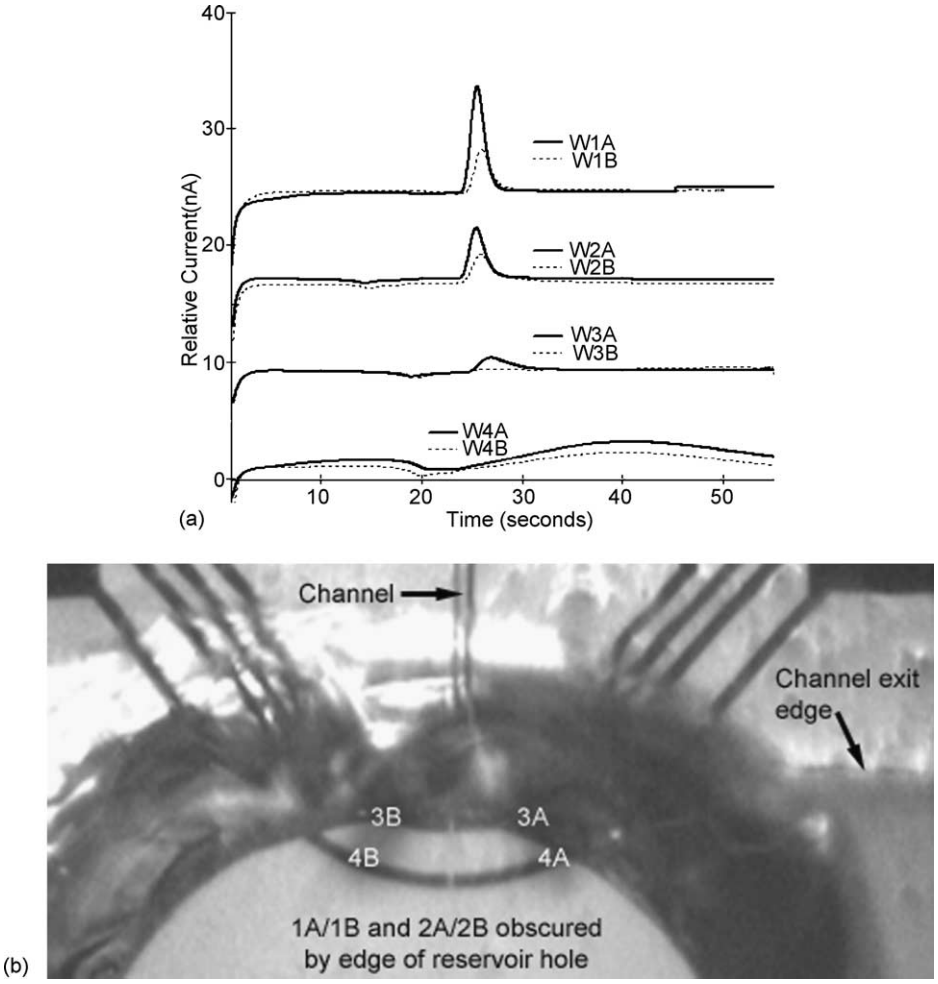

Fig. 8. Eight-electrode ED configuration when only four electrodes are under the "shelf" and four electrodes are in the reservoir: (a) dopamine output currents from all eight electrodes, and (b) photograph of the four electrode fingers (electrodes 3A/B and 4A/B) in the reservoir. *Note*: Electrodes 1A/B and 2A/B are not visible since they lie under the cut-edge of the reservoir hole.

significant diffusion of the dopamine plug had already occurred prior to detection. Certainly, the greater peak widths seen at W3B and W4B indicated the presence of some degree of diffusional band-broadening. In view of the fact that our microchips employed end-channel ED with no active decoupling, the induced effects of the HV–CE electric field on the ED potentials was another complicating issue, especially for the W1 electropherograms [49]. In principle, the electropherograms seen for both of the electrodes of each pair (i.e., W1A and W1B) would have been expected to be identical; but this was not always the case. Such differences in peak size may be attributable to slight differences in effective electrode area or even asymmetric diffusion of the analyte plug.

It is important to note that the degree of control over ED electrode placement demonstrated in Fig. 7b would be extremely difficult, if not impossible, to achieve by any other microchip construction approach. In fact, even with microfabrication, there were still critical steps in chip assembly that could greatly influence the performance of the end device. In this work, perhaps the most crucial manufacturing step proved to be the bonding of the top glass substrate (containing the CE channels) with the bottom one (containing the CE and ED electrodes). Although the photolithography process served to maintain the electrode size and spacing exactly the same from chip to chip, it was the wafer bonding process that established the orientation of the electrode pattern with respect to the CE channel. For example, Fig. 8a shows a set of electropherograms obtained for dopamine with a microchip that contained the identical eight-electrode array, as in Fig. 7b, but for which the entire electrode array was displaced 50–100 μm out from the CE channel exit. As a consequence, the W3 and W4 electrodes were located in the open detection reservoir where three-dimensional diffusion of the analyte plug was possible and very broad and weak peaks resulted [40,50].

4. Conclusion

A self-contained, transportable CE/ED analysis system with the HV and detection electrodes integrated “on-chip” has been designed, fabricated, and evaluated. State-of-the-art design/modeling methodologies and photolithographic processes have been used to control electrode placement as well as customize and develop simple, yet complex, electrode shapes directly onto the microchip platform. The results show that the analytical performance of the microfabricated devices is comparable to previously reported hybrid LOC devices with external CE and/or ED electrodes. Sample electropherograms have been successfully obtained for dopamine and catechol at mM concentrations in phosphate buffer (pH 6). Conditions: CE separation voltage = 250 V; ED potential = +0.75 V versus Pt reference electrode. The implied requirement for “on-chip” microsystems to perform multiple analyses from a single sample injection has been corroborated by the short-term results presented, suggesting the ability to do numerous quantitative analyses with an ever-decreasing quantity of original sample. It is surprising that some devices have been used in several hundreds of experiments, yet still produce nearly identical results. The long-term results indicate that, for the particular buffer and analyte used in this study, disposability of microchip devices may still be attractive, but perhaps not completely necessary. For the first time, multiple electrode array configurations have been successfully demonstrated. The majority of the electrodes (six out of eight) in the array were capable of detecting dopamine with the amplitude of the signal (i.e., peak heights) decreasing as the electrode distance from the channel exit increased.

Acknowledgements

This work was supported by the National Science Foundation XYZ-on-a-chip program under grant no. CTS-9980831, the Department of Energy under grant no. 46411101095, and the NSF EPSCoR program under grant no. 6016955.

References

[1] D.R. Reyes, D. Iossifidis, P.-A. Aurouz, A. Manz, Anal. Chem. 74 (2002) 2637.
[2] P.-A. Auroux, D. Iossifidis, D.R. Reyes, A. Manz, Anal. Chem. 74 (2002) 2653.
[3] A. Manz, N. Graber, H.M. Widmer, Sens. Actuators B: Chem. 1 (1990) 244.
[4] A. Woolley, R. Mathies, Proc. Natl. Acad. Sci. U.S.A. 91 (1994) 11348.
[5] P.C. Simpson, D. Roach, A.T. Woolley, T. Thorsen, R. Johnston, G.F. Sensabaugh, R.A. Mathies, Proc. Natl. Acad. Sci. U.S.A. 95 (1998) 2256.
[6] C.A. Emrich, H. Tian, I.L. Medintz, R.A. Mathies, Anal. Chem. 74 (2002) 5076.
[7] S.C. Jacobson, J.M. Ramsey, Anal. Chem. 69 (1997) 3212.
[8] D.P. Schrum, C.T. Culbertson, S.C. Jacobson, J.M. Ramsey, Anal. Chem. 71 (1999) 4173.
[9] V. Dolnik, S. Liu, S. Jovanovich, Electrophoresis 21 (2000) 41.
[10] J.S. Rossier, A. Schwarz, F. Reymond, R. Ferrigno, F. Bianchi, H.H. Girault, Electrophoresis 20 (1999) 727.
[11] J.P. Kutter, S.C. Jacobson, J.M. Ramsey, Anal. Chem. 69 (1997) 5165.
[12] P.C.H. Li, D.J. Harrison, Anal. Chem. 69 (1997) 1564.
[13] S.C. Jacobson, T.E. McKnight, J.M. Ramsey, Anal. Chem. 71 (1999) 4455.
[14] M. Kakuta, F.G. Bessoth, A. Manz, Chem. Record 1 (2001) 395.
[15] J.R. Webster, M.A. Burns, D.T. Burke, C.H. Mastrangelo, Anal. Chem. 73 (2001) 1622.
[16] W.R. Vandaveer IV, S.A. Pasas, R.S. Martin, S.M. Lunte, Electrophoresis 23 (2002) 3667.
[17] J. Tanyanyiwa, S. Leuthardt, P.C. Hauser, Electrophoresis 23 (2002) 3659.
[18] R.P. Baldwin, Electrophoresis 21 (2000) 4017.
[19] N.A. Lacher, K.E. Garrison, R.S. Martin, S.M. Lunte, Electrophoresis 22 (2001) 2526.
[20] J. Wang, Talanta 56 (2002) 223.
[21] A.C. Ontko, P.M. Armistead, S.R. Kircus, H.H. Thorp, Inorg. Chem. 38 (1999) 1842.

[22] C.T. Culbertson, S.C. Jacobson, J.M. Ramsey, Anal. Chem. 72 (2000) 5814.
[23] J. Wang, M.P. Chatrathi, B. Tian, Anal. Chem. 72 (2000) 5774.
[24] R.P. Baldwin, T.J. Roussel Jr., M.M. Crain, V. Bathlagunda, D.J. Jackson, J. Gullapalli, J.A. Conklin, R. Pai, J.F. Naber, K.M. Walsh, R.S. Keynton, Anal. Chem. 74 (2002) 3690.
[25] C.S. Henry, M. Zhong, S.M. Lunte, M. Kim, H. Bau, J.J. Santiago, Anal. Commun. 36 (1999) 305.
[26] J.S. Rossier, M.A. Roberts, R. Ferrigno, H.H. Girault, Anal. Chem. 71 (1999) 4294.
[27] J.S. Rossier, R. Ferrigno, H.H. Girault, Electro. Anal. Chem. 492 (2000) 15.
[28] G. Ocvirk, M. Munroe, T. Tang, R. Oleschuk, K. Westra, D.J. Harrison, Electrophoresis 21 (2000) 107.
[29] J. Wang, M. Pumera, M.P. Chatrathi, A. Escarpa, R. Konrad, A. Griebel, W. Dörner, H. Löwe, Electrophoresis 23 (2002) 596.
[30] Y. Liu, D. Ganser, A. Schneider, R. Liu, P. Grodzinski, N. Kroutchinina, Anal. Chem. 73 (2001) 4196.
[31] C.S. Effenhauser, G.J.M. Bruin, A. Paulus, M. Ehrat, Anal. Chem. 69 (1997) 3451.
[32] R.S. Martin, A.J. Gawron, S.M. Lunte, C.S. Henry, Anal. Chem. 72 (2000) 3196.
[33] A.J. Gawron, R.S. Martin, S.M. Lunte, Electrophoresis 22 (2001) 242.
[34] M.L. Chabinyc, D.T. Chiu, J.C. McDonald, A.D. Stroock, J.F. Christian, A.M. Karger, G.M. Whitesides, Anal. Chem. 73 (2001) 4491.
[35] D. Ross, T.J. Johnson, L.E. Locascio, Anal. Chem. 73 (2001) 2509.
[36] J.C. McDonald, G.M. Whitesides, Acc. Chem. Res. (2002).
[37] C.-X. Zhang, A. Manz, Anal. Chem. 73 (2001) 2656.
[38] D.C. Chen, F.L. Hsu, D.Z. Zhan, C.H. Chen, Anal. Chem. 73 (2001) 758.
[39] P. Selvaganapathy, M.A. Burns, D.T. Burke, C.H. Mastrangelo, Inline ED for Capillary Electrophoresis, 2001, p. 451.
[40] R.S. Martin, K.L. Ratzlaff, B.H. Huynh, S.M. Lunte, Anal. Chem. 74 (2002) 1136.
[41] D.M. Osbourn, C.E. Lunte, Anal. Chem. 75 (2003) 2710.
[42] A.T. Woolley, K. Lao, A.N. Glazer, R.A. Mathies, Anal. Chem. 70 (1998) 684.
[43] J. Wang, A. Ibanez, M.P. Chatrathi, A. Escarpa, Anal. Chem. 73 (2001) 5323.
[44] R.S. Martin, A.J. Gawron, B.A. Fogarty, F.B. Regan, E. Dempsey, S.M. Lunte, Analyst 126 (2001) 277.
[45] Y. Zeng, H. Chen, D.-W. Pang, Z.-L. Wang, J.-K. Cheng, Anal. Chem. 74 (2002) 2441.
[46] B.M. Paegel, L.D. Hutt, P.C. Simpson, R.A. Mathies, Anal. Chem. 72 (2000) 3030.
[47] M.M. Crain, R.S. Keynton, K.M. Walsh, T.J. Roussel Jr., R.P. Baldwin, J.F. Naber, D.J. Jackson, Microchip Capillary Electrophoresis: Methods and Protocols, Humana Press, 2003, in press.
[48] D.J. Jackson, J.F. Naber, K.M. Walsh, R.S. Keynton, T.J. Roussel Jr., M.M. Crain, R.P. Baldwin, Anal. Chem. 75 (2003) 3311.
[49] S.R. Wallenborg, L. Nyholm, C.E. Lunte, Anal. Chem. 71 (1999) 544.
[50] J.A. Lapos, D.P. Manica, A.G. Ewing, Anal. Chem. 74 (2002) 3348.